

pubs.acs.org/JACS Article

Stereoselective 1,2-cis Furanosylations Catalyzed by Phenanthroline

Hengfu Xu, Richard N. Schaugaard, Jiayi Li, H. Bernhard Schlegel, and Hien M. Nguyen*



Cite This: https://doi.org/10.1021/jacs.2c02063



ACCESS

III Metrics & More

Article Recommendations

Supporting Information

ABSTRACT: Stereoselective formation of the 1,2-cis furanosidic linkage, a motif of many biologically relevant oligosaccharides and polysaccharides, remains an important synthetic challenge. We herein report a new stereoselective 1,2-cis furanosylation method promoted by phenanthroline catalysts under mild and operationally simple conditions. NMR experiments and density functional theory calculations support an associative mechanism in which the rate-determining step occurs from an inverted displacement of the faster-reacting phenanthrolinium ion intermediate with an alcohol nucleophile. The phenanthroline catalysis system is applicable to a number of furanosyl bromide donors to provide the challenging 1,2-cis substitution products in good yield with high anomeric selectivities. While arabinofuranosyl bromide provides β -1,2-cis products, xylo- and ribofuranosyl bromides favor α -1,2-cis products.

$$(BnO)_{n} \xrightarrow{O}_{2} \stackrel{1}{1} + ROH \xrightarrow{5 \text{ mol}\% \text{ BPhen}} \stackrel{(BnO)_{n}}{}_{0} \xrightarrow{O}_{2} \stackrel{1}{}_{1} + ROH \xrightarrow{5 \text{ mol}\% \text{ BPhen}} \stackrel{(BnO)_{n}}{}_{0} \xrightarrow{Ci}_{0} \stackrel{Ci}{}_{0} \stackrel{Ci}$$

INTRODUCTION

The interest in the stereoselective synthesis of furanose-containing glycans has been growing rapidly over the past decade ^{1–6} as furanoses are key constituents of many pathogenic microorganisms and plants. Oligosaccharides and polysaccharides containing 1,2-trans and 1,2-cis furanosidic linkages (Figure 1) are generally present in the cell walls of the microorganisms and play critical roles in disease progression and interaction with the host immune system. As a result, they are targets for therapeutic intervention. The 1,2-trans furanosides are obtained through neighboring group participation of the C2-O-acyl protecting group. On the other hand, the ability to access 1,2-cis furanosides requires furanosyl donors with a nonassisting functionality at C2. The use of these electrophilic donors often leads to the formation of a mixture of two stereoisomers that differ in the configuration of the anomeric center.

The furanosides react closer to the $S_{\rm N}1$ end of the $S_{\rm N}1-S_{\rm N}2$ boundary than their pyranoside counterparts due to their conformational flexibility and electronic properties. To overcome these inherent challenges, several groups have employed conformationally blocked furanosyl donors that provide 1,2-cis furanosides with high levels of anomeric selectivity. The introduction of 1,2-cis-furanosidic linkages has also been achieved by indirect protocols, including intramolecular aglycon delivery, emote participation of the acyl protecting group at C3 or C5, 23,24 hydrogen bonding-assisted coupling, and regioselective opening of the 2,3-anhydrofuransoyl donor. While these substrate-controlled methods have been successful in providing solutions to a number of 1,2-cis furanosylation challenges in the oligosaccharide synthesis, 28–34 achieving the desired stereoselectivity

remains system-dependent. Subtle changes to the structure of carbohydrate coupling partners have pronounced effects on the furanosylation selectivity and reactivity.

Methods that enable catalytic stereoselective glycosylation are a powerful means of rapidly introducing 1,2-cis furanosidic linkages into biologically relevant oligosaccharides, obviating the need to rely on substrate control. Catalysis with small organic molecules to expand the chemical space of the stereoselective 1,2-cis furanosylation reaction is of interest. The area of organocatalysis has become a highly dynamic area of research, as small organic molecules are capable of catalyzing a wide range of organic reactions. 35-46 Recently, Jacobsen and co-workers reported the use of small-molecule catalysts, bis-thiourea hydrogen-bond donors, to mediate the formation of 1,2-cis furanosides in high yields and stereoselectivities.⁴⁷ In their investigation, 1,2-trans furanosyl phosphate donors undergo substitution with a variety of hydroxyl acceptors to provide access to 1,2-cis products.⁴⁷ However, when a β -1,2-trans xylofuranosyl phosphate donor (cis/trans = 1:11) was employed in the reaction (Figure 2), the β -1,2-trans product was obtained as the major product with the net retention of anomeric configuration (cis/trans = 1:13).⁴⁷ This is a unique case when compared to other furanosyl phosphates under bis-thioureacatalyzed selective furanosylation conditions.

Received: February 22, 2022



Figure 1. Hexasaccharide motifs found in the cell wall complex of mycobacterial arabinogalactan (AG) and lipoarabinomannan (LAM). Araf = arabinofuranose and Xylf = xylofuranose.

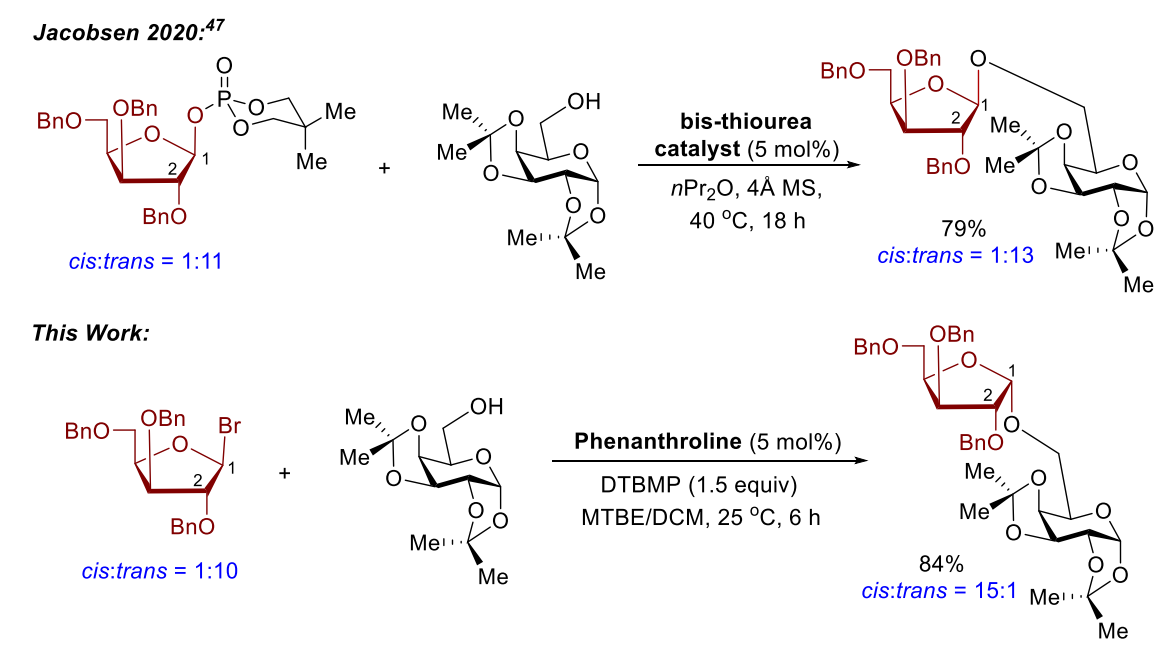


Figure 2. Catalytic stereoselective xylofuranosylation.

Our group recently discovered that phenanthroline, a rigid and planar organic compound with two pyridine rings fused to a benzene ring, effectively acts as a nucleophilic catalyst to promote the stereoselective glycosylation with α -pyranosyl bromide donors providing α -1,2-cis pyranosides with net retention of the anomeric configuration. 48-50 The reaction is governed by Curtin-Hammett principles and proceeds through the more reactive β -pyranosyl phenanthrolinium ion intermediate. The α -1,2-cis selectivity is rationalized by a model in which a nucleophilic attack takes place from the α -face of the β glycosyl phenanthrolinium ion. 50 Given the paucity of catalytic stereoselective 1,2-cis furanosylation reports, we saw an opportunity to demonstrate the utility of our catalytic strategy toward furanose substrates. Herein, we report the commercially available phenanthroline-catalyzed stereoselective glycosylations of a variety of hydroxyl nucleophiles with furanosyl

bromide donors to provide access to the challenging 1,2-cis furanoside products with high levels of anomeric selectivity. Unlike pyranose substrates, the reaction with furanose substrates proceeds with an inversion of stereochemistry. As illustrated in Figure 2, reaction of 1,2:3,4-di-O-isopropylidene- α -D-galactopyranoside with the β -1,2-trans xylofuranosyl bromide donor (cis/trans = 1:10) using 5 mol % 4,7-diphenyl-1,10-phenanthroline with respect to the bromide provided the α -1,2-cis product with excellent selectivity (cis/trans = 15:1). This result is the opposite of Jacobsen's observation (Figure 2). The phenanthroline catalysis system has also been extended to a number of furanosyl bromide donors. While arabinofuranosyl bromide provides β -1,2-cis products as the major stereoisomers, xylo- and ribofuranosyl donors favor α -1,2-cis products.

Table 1. Effect of Reaction Parameters a,b,c

BnO OBn Br Me OH DTBMP (1.5 equiv) Me Me Standard conditions
$$\frac{1}{\alpha \cdot \beta} = 1:10$$

entry variation from the "standard" condtions $\frac{1}{\alpha}$ (%) ratio $\frac{1}{\alpha}$ 1 none 84 15:1

entry variation from the "standard" condtions			yield ^b (%)	α:β ratio ^c	
1	none			84	15:1
2	IBO, instead of DTBMP			76	10:1
3	no BPhen and no DTBMP			28	1:1
4	no BPhen, 15 mol% DTBMP only			35	3:1
5	no BPhen, 1.5 equiv. DTBMP only			56	6:1
6	no BPhen, 1.0 equiv. AgOT		50	4:1	
7	THF as solvent		64	9:1	
8	Et ₂ O as solvent		59	11:1	
9	MTBE as solvent		68	15:1	
10	CH ₂ Cl ₂ as solvent			90	11:1
11	NPhen instead of BPhen			81	15:1
12	1,10-Phenanthroline instead of BPhen			61	13:1
13	4-Phenylpyridine instead of BPhen			49	10:1
14	Benzo[h]quinoline instead of BPhen			44	11:1
$\begin{array}{c c} & & & & \\ & & \\ & & & \\ & & \\ & & & \\ & & & \\ & & & \\ & & & \\ & & & \\ & & & \\ & & & \\ & & & \\$		O Me Me	Me t-Bu N t-Bu		
В	Phen NPher	1	IBO	D	ТВМР

"All furanosylations were conducted with 1 (0.6 mmol), 2 (0.2 mmol), and 5 mol % of the catalyst with respect to the donor 1 in a 5:1 mixture of MTBE/CH₂Cl₂ (0.2 M). "Yield of isolated 3 averaged over two to three runs." Diastereoselectivity (α/β) was determined by "H NMR.

4-Phenylpyridine

RESULTS AND DISCUSSION

In our previously reported pyranosylation reaction, we discovered that phenanthroline was the most effective catalyst to give rise to the α -1,2-cis pyranosides with high yield and excellent anomeric selectivity. We proposed to explore this chemistry to the furanosylation reaction, although we anticipated some challenges associated with the more flexible furanose substrates. In the pursuit of phenanthroline-catalyzed stereoselective formation of 1,2-cis furanosidic linkages, we selected xylosyl bromide 1 (Table 1) as a donor so that we can compare the reaction outcome to the previous methods to further gain insight into the reaction mechanism. Because it is

1,10-Phenanthroline

difficult to obtain β -isomer of donor 1 in a pure form, a 10:1 β/α mixture of 1 with β -1,2-trans isomer as a major starting material was used to evaluate with a variety of combinations of phenanthroline catalysts, pyridine catalysts, acid scavenger, and solvents. Through optimization, we established that furanosylation of galactopyranoside alcohol acceptor 2 with furanosyl bromide 1 using 5 mol % of commercially available 4,7-diphenyl-1,10-phenanthroline (BPhen) with respect to donor 1 and di-tert-butylmethylpyridine (DTBMP) as an acid scavenger in a 5:1 mixture of MTBE and CH₂Cl₂ solvent at 25 °C for 6 h afforded the 1,2-cis xylofuranoside product 3 in good yield (84%) and excellent diastereoselectivity ($\alpha/\beta=15:1$, Table 1, entry 1). Control experiments revealed that the BPhen

Benzo[h]quinoline

Six-Membered Ring Carbohydrate Acceptors

Five-Membered Ring Carbohydrate Acceptors

Complex Steroid Acceptors Me Me Me Me Me Me H CO₂Me Me Me H CO₂Me Dexamethasone (11) Cholestanol (12) Oleanolic Acid (13)

Figure 3. Carbohydrate and complex steroid nucleophiles.

catalyst and a stoichiometric amount of acid scavenger (DTBMP) are essential to achieving good yield and high levels of anomeric selectivity (entries 2-5). For instance, the use of isobutylene oxide (IBO) instead of DTBMP as an electrophilic trap of HBr reduced both yield and cis/trans diastereoselectivity $(84 \rightarrow 76\%, 15:1 \rightarrow 10:1, entries 1 vs 2)$. Interestingly, the reaction proceeded even in the absence of both BPhen catalyst and DTBMP to provide disaccharide 3 in low yield (28%) with no anomeric selectivity (entry 3), presumably due to product decomposition in the absence of the acid scavenger. Use of 15 mol % of DTBMP provided disaccharide 3 in 35% yield with α / β = 3:1 (entry 4). Further increasing the amount of DTBMP to 1.5 equiv improved both yield and selectivity of 3 (35 \rightarrow 56%, $3:1 \rightarrow 6:1$, entries 4 vs 5). We hypothesize that utilizing DTBMP would not only sequester the HBr byproduct but also preserve bromide ions in the reaction to promote the coupling. 50,51 However, the bromide-mediated xylosylation reaction is not as effective as the BPhen catalyst (entry 1 vs 5). We also conducted the coupling of 2 with 1 employing a standard silver triflatemediated coupling protocol (entry 6), and disaccharide 3 was obtained in 50% yield as a 4:1 mixture of α - and β -isomers. Although the use of ethereal solvents proved critical (entries 7– 10), the use of dichloromethane solvent improved the yield of 1,2-cis product 3 due to increased solubility (entry 10). While synthetically prepared 4,7-piperidine-substituted phenanthroline (NPhen) was more effective than BPhen to mediate the formation of α -1,2-cis pyranosides,^{49,50} it did not affect the outcome of the furanosylation reaction (entry 11). The nonsubstituted phenanthroline catalyst (entry 12) reduced both reaction selectivity and reactivity. To determine the role of the dual pyridine system displayed in the phenanthroline framework, we evaluated the 4-phenyl-pyridine catalyst (entry 13) and a reduced yield (49%) and anomeric selectivity (α/β = 10:1) were obtained in comparison to the BPhen catalyst (entry 1). Finally, to confirm the critical role of the C2 symmetry on phenanthroline, benzo[h]quinoline (entry 14) containing only one pyridine ring was evaluated. The result revealed that this

catalyst is less reactive and selective compared to BPhen bearing two pyridine rings (entry 1), further validating the importance of the second pyridine nitrogen atom on the phenanthroline framework. For comparison, furanosylation of primary alcohol 2 with xylofuranosyl thioglycoside donor bearing a conformationally constrained xylene protecting group afforded the desired 1,2-cis xylofuranoside product in 73% yield with $\alpha/\beta = 9.5:1.$ ¹⁹

The acceptor scope (Figure 3), including primary and secondary hydroxyls of pyranoside (4-6), furanoside (7-10), and structurally complex triterpenes (11-13), was next examined (Table 2) using xylofuranosyl bromide 1 and the BPhen catalyst. The results were uniformly excellent, providing the coupling products 14-23 (Table 2) in good yields (55-90%) and excellent α -1,2-cis selectivity ($\alpha/\beta = 15:1-20:1$). For instance, the coupling of C6-hydroxyl of pyranoside acceptors 4 and 5 with xylofuraosyl bromide donor 1 provided disaccharides 14 and 15, respectively, in 72–90% yield with $\alpha/\beta = 17:1$. We also conducted the coupling in the absence of the BPhen catalyst, and disaccharide 15 was obtained in 51% yield with significantly lower anomeric selectivity ($\alpha/\beta = 6:1$). Use of the standard AgOTf activation protocol provided 15 in much lower yield and α -selectivity (59%, $\alpha/\beta = 3:1$) compared to the reaction with BPhen catalyst. On the other hand, furanosylation of nucleophilic acceptor 5 with xylosyl thioglycoside donor bearing a conformationally blocked xylene protecting group afforded the desired disaccharide with $\alpha/\beta = 7.8:1.^{19}$ Similar stereochemical outcome was observed with the use of the sterically hindered C4-hydroxyl of pyranoside acceptor 6, affording the desired 1,2-cis product 16 in 58% yield with excellent anomeric selectivity ($\alpha/\beta = 15:1$) under phenanthroline-catalyzed conditions. The presence of electron-donating (Bn) and -withdrawing (Bz) groups on primary and secondary alcohols of furanoside acceptors 7-10 had little effect on the reaction selectivity, providing disaccharides 17-20 with excellent diastereoselectivity ($\alpha/\beta = 15:1-20:1$); a slight decrease in yield was observed with secondary alcohols 9 and 10 forming disaccharides 19 and 20, respectively. To compare,

Table 2. Reaction of Alcohol Nucleophiles with p-Xylofuranosyl Bromide a,b,c,d,e,f,g,h

^aAll furanosylations were conducted with xylofuranosyl bromide 1 (0.6 mmol), alcohol acceptors (0.2 mmol), and 5 mol % of BPhen with respect to the donor 1 in a 5:1 mixture of MTBE/CH₂Cl₂ (0.2 M). ^bIsolated yield. ^cDiastereoselectivity (α/β) was determined by ¹H NMR. ^dThe reaction was stirred at 25 °C for 6 h. ^eThe reaction was stirred at 25 °C for 12 h. ^fThe reaction was conducted with 5 mol % BPhen and 1.5 equiv of DTBMP for 6 h. ^gThe reaction was conducted with 1 equiv of AgOTf and 1.5 equiv of DTBMP for 12 h.

the coupling of primary and secondary alcohol-containing furanoside acceptors with the conformationally blocked thioglycoside donor afforded the xylosylated products with α / $\beta \sim 7.5:1.^{19}$ The phenanthroline-catalyzed method is not limited to carbohydrate acceptors as functionally complex steroids 11-13 (Table 2) proved to be efficient nucleophiles. For instance, furanosylation of the preferred primary hydroxyl site of dexamethasone 11, an anti-inflammatory and immunosuppressive corticosteroid that has been used as the drug to treat severe COVID-19 patients, 52 with xylofuranosyl bromide 1 afforded the 1,2-cis product 21 in 83% yield and excellent α -selectivity $(\alpha/\beta = 16:1)$. Next, we evaluated the catalytic furanosylation reaction with cholestanol 12, affording the coupling product 22 in high yield and selectivity (89%, α/β = 12:1). We were pleased to find that the coupling of oleanolic acid methyl ester 13, a potential therapeutic agent to improve insulin action, inhibit gluconeogenesis, and promote glucose utilization, 53 with donor 1 could be achieved to afford the desired conjugate 23 in 55% yield with 15:1 cis/trans diastereoselectivity.

Motivated by the efficiency of the phenanthroline-catalyzed furanosylations with D-xylofuranosyl bromide donor 1, we next investigated the coupling of pyranoside and furanoside nucleophiles with D-arabinofuranosyl bromide donor 24. Because it is challenging to obtain arabinosyl bromide in a high α -form, a 7:1 α/β mixture of starting material 24 with α -1,2-trans isomer as the major donor was subjected to the optimal coupling conditions with nucleophilic acceptors (Table 3). In all cases, the reactions proceeded in good to excellent yields with nearly complete inversion of the stereochemistry at the anomeric configuration. For example, the reaction of primary alcohols of pyranoside acceptors 2, 4, and 5 afforded the corresponding arabinofuranoside products 25-27 in 78-90% yield with *cis/trans* ratio of ~1:8, favoring the β-1,2-*cis* isomers. Similarly, reactions of primary and secondary alcohols of furanoside acceptors 7–10 afforded β -1,5-, β -1,3- and β -1,2-cis linked arabinofuranosides 28-31 in good yields (61-85%) and anomeric selectivity ($\alpha/\beta = \sim 1.8$). We also observed that the selectivity of the newly formed furanosidic linkage is not dependent on the reactivity of a nucleophilic acceptor as both

Table 3. Reaction of Alcohol Nucleophiles with D-Arabinofuranosyl Bromide a,b,c,d,e,f

"All furanosylations were conducted with arabinofuranosyl bromide 24 (0.6 mmol), alcohol acceptors (0.2 mmol), and 5 mol % of BPhen with respect to the donor 24 in a 5:1 mixture of MTBE/CH₂Cl₂ (0.2 M). "Isolated yield. "Diastereoselectivity (α/β) was determined by ¹H NMR. "The reaction was conducted with 5 mol % BPhen and 1.5 equiv of DTBMP for 6 h. "The reaction was conducted with 1.5 equiv of DTBMP only for 12 h. "The reaction was conducted with 1 equiv of AgOTf and 1.5 equiv of DTBMP for 12 h.

electron-withdrawing 9 and -donating 10 acceptors provided 30 and 31, respectively, with similar β -selectivity ($\alpha/\beta = 1.8$, Table 3). Increases in yield and β -anomeric selectivity (e.g., 27) were observed under the phenanthroline-catalyzed conditions when compared to the standard AgOTf activation protocol or the reaction mediated by the stoichiometric amount of acid scavenger, DTBMP, only (Table 3). It has been reported that the stereoselective β -arabinofuranosylation employing a 2'carboxybenzyl arabinofuranosyl donor is highly acceptordependent as the electron-withdrawing group on a nucleophile is necessary to achieve β -1,2-cis selectivity. ²⁴ In contrast, the use of the electron-donating benzyl group on furanoside acceptor (e.g., 10) in the reaction with 2'-carboxybenzyl arabinofuranosyl donor provided disaccharide 31 with poor anomeric selectivity $(\alpha/\beta = 1:2.2)^{24,27}$ This limitation associated with the preparation of 31 is overcome by the phenanthroline catalytic method ($\alpha/\beta = 1:8$).

In addition to xylosyl (1) and arabinosyl (24) bromide donors, we next sought to evaluate the performance of other furanosyl donors under BPhen-catalyzed furanosylation conditions (Scheme 1). In all cases, 5 mol % of BPhen was employed in the reaction with respect to the donor. Ribofuranosyl bromide 32—the C3 epimer of xylosyl donor 1—was first utilized in the reaction. Like arabinosyl bromide 24 (Table 3), we were unable to obtain ribofuranosyl bromide 32 in a high β -form. As a result, a 1:7 α/β mixture of 32, with β -1,2-trans isomer being the major starting material, was subjected to the phenanthroline-catalyzed coupling conditions with pyranoside nucleophile 2 as well as furanoside nucleophiles 7 and 9 (Scheme 1a—c). Again, inverted substitution was observed in all examples. Good yields (60–90%) and selectivity ($\alpha/\beta \sim 7:1$) were obtained for the desired

α-1,2-cis products 33–35 (Scheme 1a–c). Our catalytic reaction is comparable to the bis-thiourea-catalyzed furanosylation when an α/β mixture of ribofuranosyl phosphate was used to test the effect of donor anomeric composition ($\alpha/\beta=8:1$). Overall, ribofuranosyl bromide donor 32 is less α-selective than xylofuranosyl bromide 1 (see Tables 1 and 2). Next, L-arabinosyl bromide 36 was employed as a donor in the reaction with primary pyranoside acceptor 5 (Scheme 1d). We found that L-arabinosyl bromide 36 reacted similarly to D-arabinosyl bromide 24 (Table 3, 27: 88%, $\alpha/\beta=1:8$) to yield disaccharide 37 in 86% yield with good *cis/trans* diastereoselectivity ($\alpha/\beta=1:8$). To compare, furanosylation of pyranoside acceptor 5 with L-arabinosyl thioglycoside donor, promoted by the reagent combination of NIS/AgOTf, provided 37 in 88% yield with $\alpha/\beta=1:3$.

To determine the effect of the conformationally constrained donor on reaction selectivity under BPhen-catalyzed conditions, we conducted the coupling of pyranoside acceptor 4 with 3,5-O-(di-tert-butylsilyl)-2-O-benzylarabinofuranosyl bromide 38 (Scheme 1e); disaccharide 39 was obtained in 76% yield with α/β = 1:4 (Scheme 1e), a decrease in anomeric selectivity compared to the unconstrained arabinofuranosyl bromide donor (26: 90%, $\alpha/\beta = 1:8$, Table 3). This experiment suggests that a free arabinofuranosyl donor 24 is more suited under our BPhen catalytic conditions. In the early work reported by Imamura and Lowary, the coupling of primary alcohol 4 with a conformationally restricted 2,3-O-xylylene arabinofuranosyl thioglycoside promoted by NIS/AgOTf activation protocol provided the coupling product with similar selectivity (α/β = 1:5)17 to that with a conformationally blocked furanosyl bromide donor 38 catalyzed by BPhen. On the other hand,

BnO

Scheme 1. Furanosyl Donor Scope

the coupling of alcohol acceptor 4 with unconstrained thioglycoside derivative of 38 using the reagent combination of 1-benzenesulfinyl piperidine and triflic anhydride provided 39 almost as a $1:1~\alpha/\beta$ mixture. ¹⁵

Unlike other furanosyl donors, the coupling of pyranoside acceptor 4 with α -lyxofuranosyl bromide donor 40 (α/β = 20:1, Scheme 1f) under phenanthroline-catalyzed conditions provided the desired disaccharide 41 in 88% yield but with poor

Scheme 2. Donor Anomeric Composition

(a) BnO
$$\frac{1}{1000}$$
 Br $\frac{1}{1000}$ Br $\frac{1}$

anomeric selectivity ($\alpha/\beta=1:2$). To compare, the lyxofuranosyl phosphate donor was completely unreactive with bis-thiol urea catalysts. ⁴⁷ Importantly, this result suggests that donor anomeric composition has no significant impact on the stereochemical outcome of furanosylation. Further, this experiment suggests that the orientation of the C3-oxygen substituent exerts a powerful effect upon reaction selectivity. For example, arabinofuranosyl bromide 24—the C3 epimer of lyxofuranosyl bromide 40—was found to be more β -selective (26, $\alpha/\beta=1:8$, Table 3).

Jacobsen and co-workers have reported that the anomeric composition of the furanosyl phosphate donors had a pronounced effect on the reaction outcome under bisthiourea-catalyzed furanosylation conditions.⁴⁷ For example, the coupling of alcohol acceptor 2 with α -arabinofuranosyl phosphate provided disaccharide 25 with $\alpha/\beta = 1.25.47$ In contrast, the use of an 8:1 α/β mixture of arabinofuranosyl phosphate donor led to a decrease in selectivity, affording 25 with $\alpha/\beta = 1:10$, which is comparable with our BPhen catalysis conditions ($\alpha/\beta = 1.7$, Table 3). Since we were unable to obtain α -D-arabinofuranosyl bromide **24** in a high α -form, it is unclear how the anomeric composition of this donor could impact the stereochemical outcome under phenanthroline-catalyzed furanosylation conditions and whether the furanosylation operates by associative mechanisms. 48-50 To determine if the stereochemical outcome of the reaction is dependent on the anomeric configuration of the electrophilic partner, we proposed to replace the C2-oxygen of arabinose with a fluorine atom to generate 2-fluoro-arabinofuranosyl bromide since this donor has been obtained with high α -selectivity. ⁵⁴ As anticipated, 2-fluoro arabinosyl bromide 42 (Scheme 2) was primarily isolated as the α -furanosyl donor (α/β = 20:1). Although the reaction of donor 42 with primary alcohol acceptor 2 provided disaccharide 43 in 71% yield (Scheme 2a), a decrease in β -1,2-cis selectivity (α/β = 1:5) was observed in comparison to the result obtained for a 7:1 α/β mixture of arabinofuranosyl bromide donor 24 ($\alpha/\beta = 1.7$, Table 3). Interestingly, similar anomeric selectivity ($\alpha/\beta = 1.5$) was also obtained for 1,2-cis product 43 in the coupling of alcohol 2 with 2-fluoro arabinosyl phosphate mediated by the bis-thiourea catalyst. 47 Next, we replaced the C2-oxygen of xylose with a fluorine atom to form 2-fluoro xylofuranosyl

bromide donor 44 (Scheme 2b). Interestingly, while donor 44 was primarily isolated as a 1:1 α/β mixture, the coupling product 45 was obtained with excellent levels of *cis/trans* diastereoselectivity ($\alpha/\beta=17:1$). Taken together, the data obtained in Scheme 2 suggest that furanosyl donor anomeric composition is not responsible for the reaction anomeric selectivity.

The use of 2-fluorofuranosyl bromide donors 42 and 44 (Scheme 2) also allows us to study the effect of C2-fluorine atom on the reaction selectivity as the directing role of fluorine at C2 on 1,2-trans glycosylation with pyranosyl donors has been reported. Two mechanistic S_N1 and S_N2 scenarios have been proposed. For the S_N1 pathway, the C2-F bond of pyranosyl donor adopts a quasi-axial arrangement to allow maximum orbital overlap for $\sigma_{\text{C-F}}^*$ and the incoming alcohol nucleophile in the transition state. As such, if the C2-fluorine directs furanosylation, 1,2-trans products should be obtained as the major products. However, in both the phenanthroline system and the bis-thiourea system, 47 1,2-cis products 43 and 45 (Scheme 2) were observed as the major products, suggesting either the reaction did not undergo the S_N1 pathway or the catalyst overrides the C2-fluorine directing effect. For the S_N2 pathway, it has been proposed that the C2-fluorine may induce an electrostatic attraction between the pyranosyl donors and alcohol nucleophiles. 55 If the reaction proceeds through the S_N2 pathway, the final coupling product should be in the opposite stereochemistry of the glycosyl electrophile. In the 2-fluoroarabinofuranosylation case, we used furanosyl bromide 42 with 20:1 of α/β ratio but only obtained 1:5 of α/β ratio for the coupling products 43 (Scheme 2a). On the other hand, in the 2fluoro-xylofuranosylation case, although a 1:1 anomeric mixture of furanosyl bromide 44 was used in the reaction, a high α/β ratio (17:1) of the coupling product 45 (Scheme 2b) was obtained. These results suggest that the furanosylation does not undergo a direct S_N2 pathway. The data are also consistent with our recent report on the phenanthroline-catalyzed stereoselective construction of 2-fluoropyranosides, in which the phenanthroline catalyst overrides the C2-fluorine directing effect and gives access to the corresponding α -1,2-cis-2fluoropyranosides.4

With the possibility that the reaction goes through covalent phenanthrolinium ion intermediates, NMR spectroscopy was

Scheme 3. NMR Detection of Phenanthroline-Catalyzed Reaction with Furanosyl Bromides

Figure 4. Reaction progress of phenanthroline-catalyzed xylofuranosylation of alcohol acceptor 2 using ¹⁹F NMR: (a) xylofuranosyl bromide 44 and products 45; (b) xylofuranosyl-phenanthrolinium intermediates $\operatorname{Int}_1(\beta)$ and $\operatorname{Int}_2(\alpha)$.

ı

0.01

0

0

2

0.005

employed to detect the putative intermediates. To minimize the proton signals on the aromatic region, NPhen was chosen as a catalyst of choice. In addition, both 2-fluoro xylosyl 42 and arabinosyl 44 bromides were chosen as model donors in our NMR study, as we have established their anomeric composition (see Scheme 2).

2

4

Time (h)

6

0.06

0.04

0.02 0

0

With the previous knowledge that the covalent phenanthrolinium ion intermediates form within 30 min upon combining the pyranosyl donor with NPhen, 50 the first step in our study was to add NPhen (0.13 mmol) to the 1:1.25 α/β mixture of 2-fluoro xylofuranosyl bromide 44 (0.10 mmol) at 25

°C. Within 1 h, new signals appeared around the phenanthroline region (7.0-9.1 ppm) and the sugar region (5.4-6.0 ppm) (Figure S3). An aliquot of the reaction mixture was then analyzed by electrospray ionization (ESI) mass spectrometry with an m/z ratio of 661.3548 (Figure S6), confirming the formation of the phenanthrolinium ion. Furthermore, the number of new signals in both ¹H and ¹⁹F NMR indicates that there are two possible intermediates, Int₁ and Int₂, present in a ratio of 2:1 in the reaction (Scheme 3a and Figures S3-S5). In ¹H-¹H COSY and ROESY NMR analysis (Figures S7-S8), the C1 protons of the anomeric mixture of Int, and Int, were

4

Time (h)

6

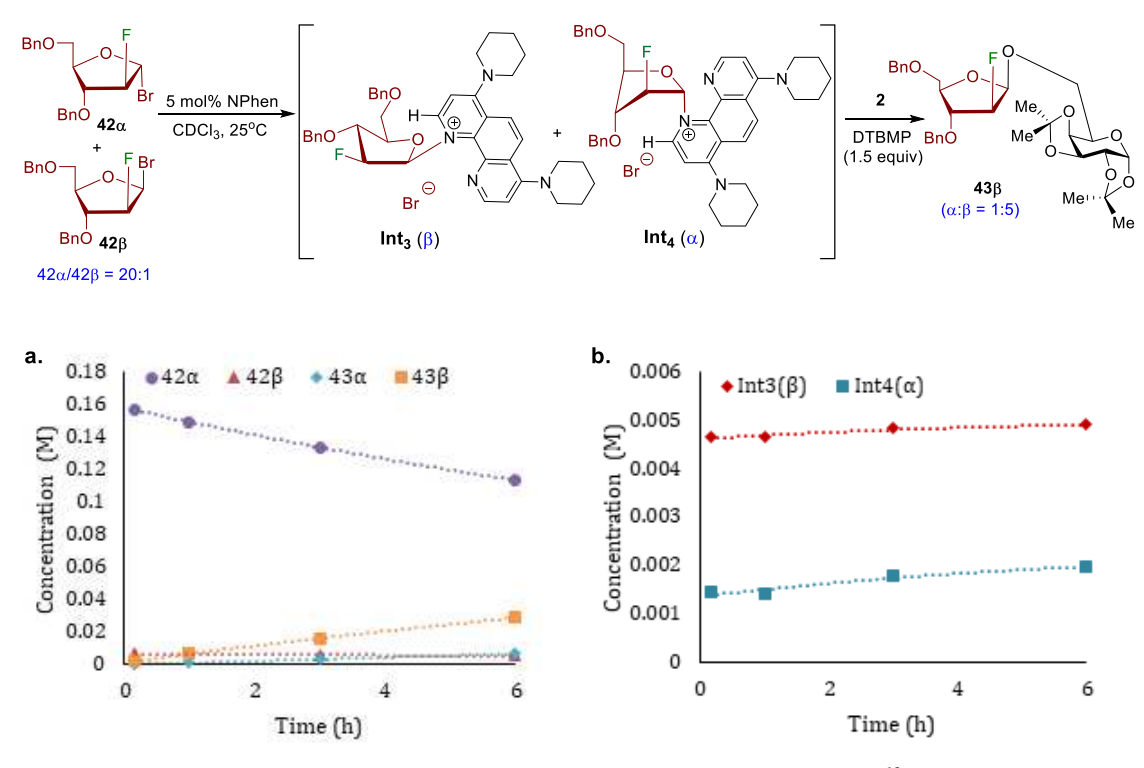


Figure 5. Reaction progress of phenanthroline-catalyzed arabinofuranosylation with alcohol acceptor 2 using ^{19}F NMR: (a) arabinofuranosyl bromide 42 and coupling products 43; (b) arabinofuranosyl-phenanthrolinium intermediates $Int_3(\beta)$ and $Int_4(\alpha)$.

identified to reside at $\delta_{\rm H}$ = 7.63 and 8.02 ppm, respectively. On the other hand, the C2-fluorine of ${\bf Int_1}$ and ${\bf Int_2}$ resides at $\delta_{\rm F}$ = -188.01 ppm (ddd, J = 45.7, 16.1, 8.4 Hz) and $\delta_{\rm F}$ = -189.64 ppm (ddd, J = 52.2, 17.9, 14.0 Hz), respectively, in the ¹⁹F NMR (Figure S4). Through 2D ROESY NMR analysis, the major ${\bf Int_1}$ was identified as a β -phenanthrolinium ion and existed in the ³E envelop conformation, while the minor ${\bf Int_2}$ was an α -phenanthrolinium ion and adopted the E₃ envelop conformation (Scheme 3a and Figures S5 and S8).

In the case of 2-fluoro arabinofuranosyl bromide 42 ($\alpha/\beta=20:1$, Scheme 3b), our NMR study of the 1:1 stoichiometry ratio of donor 42 and NPhen mixture shows that two key intermediates, a major 3E β -phenanthrolinium ion conformer (Int₃) and a minor E_3 α -phenanthrolinium ion conformer (Int₄), were also formed in a ratio of 2:1 β/α mixture (Figures S11–S13). The formation of the arabinosyl phenanthrolinium ion intermediate was also confirmed using electrospray ionization (ESI) with an m/z ratio of 661.3541 (Figure S14). From the 2D NMR study (Figures S15 and S16), the C1 protons of the anomeric mixture of Int₃ and Int₄ were identified to reside at $\delta_{\rm H}=7.99$ ppm and $\delta_{\rm H}=8.05$ ppm, whereas the C2-fluorine resides at $\delta_{\rm F}=-192.53$ ppm (ddd, J=51.3, 20.5, 11.8 Hz) and $\delta_{\rm F}=-186.34$ ppm (dt, J=46.0, 13.3 Hz), respectively (Figure S12).

Collectively, the discovery of both α/β intermediates in the NMR study further illustrates that the phenanthroline-catalyzed furanosylation does not proceed through a stereospecific substitution. However, to obtain high levels of 1,2-cis selectivity, the reaction is likely to proceed through a Curtin–Hammett scenario, wherein interconversion of the β -phenanthrolinium intermediate and its α -conformer must be more rapid than nucleophilic addition of alcohol acceptor. To further investigate this potential mechanism, we next performed a reaction progress analysis using NMR spectroscopy.

In the reaction progress analysis, both 2-fluoro xylose 44 and arabinose 42 were again chosen as furanosyl bromide donors (0.3 M), and primary alcohol 2 (0.1 M) was chosen as the acceptor since we have established the α/β selectivity of the resulting products 45 and 43 (Scheme 2). The reactions were carried out in deuterated chloroform (CDCl₃) with 5 mol % NPhen with respect to the bromides and 1.5 equiv of DTBMP as the acid scavenger. Taking advantage of the C2-fluorine, the reaction progress was monitored using ¹⁹F NMR for 20–24 h, and the relative concentrations of furanosyl bromide, covalent phenanthrolinium intermediates, and the disaccharide products were then determined (see Figures 4 and 5 as well as the Supporting Information (SI)).

First, we monitored the reaction progress of 2-fluoro xylofuranosyl bromide donor 44 ($\alpha/\beta = 1/1.25$) 30 min after mixing 44 with 5 mol % NPhen using both ¹H (Figure S1) and ¹⁹F (Figure S2) NMR. Interestingly, $Int_1(\beta)$ and $Int_2(\alpha)$ appeared with a ratio of 1:8 (Figure S2). After alcohol acceptor 2 had been added to the reaction mixture for 1 h, a new sharp fluorine signal residing at $\delta_{\rm F} = -204.18$ ppm (dd, J = 52.9, 16.2) Hz) was verified to be the disaccharide 45 (α -isomer, Figure S2). Meanwhile, an indistinct fluorine peak located at $\delta_{\rm F} = -193.02$ ppm (ddd, J = 50.2, 17.5, 14.3 Hz) was later confirmed to be the β -isomer of 45 (Figure S2). Overall, the α/β selectivity of the disaccharides 45 was determined to be 21:1 after 24 h. The reaction progress analysis of xylofuranosyl donor 44 and alcohol acceptor 2 was also quantified as a kinetic profile in a concentration vs time graph (Figure 4). The linear relationship between the concentrations and time in the kinetic profile (Figure 4a) revealed that the xylofuranosylation was in apparent zero-order kinetics in the first 7 h. Interestingly, although the anomeric mixture of xylofuranosyl bromides disappeared at similar rates, the two products appeared at significantly different rates—the rate of 45α formation was 16 times faster than that of

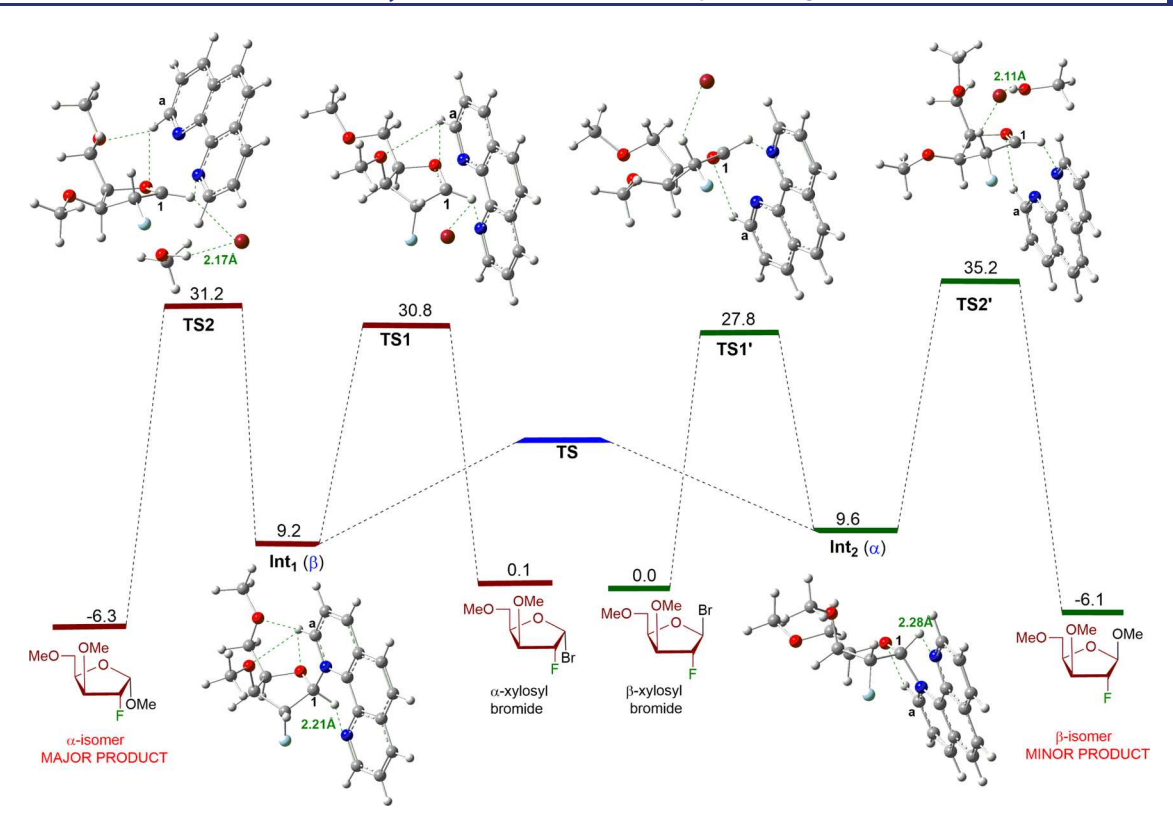


Figure 6. Energetic profile of the 2-fluoro-xylofuranose substrate. Oxygen = red, nitrogen = blue, bromine = maroon, and fluorine = light blue. Hydrogen bonding interaction (green line). Free energies (kcal/mol) were computed with the Gaussian 16 quantum chemical program package 56 using the hybrid exchange—correlation functional M06-2X. 57,58

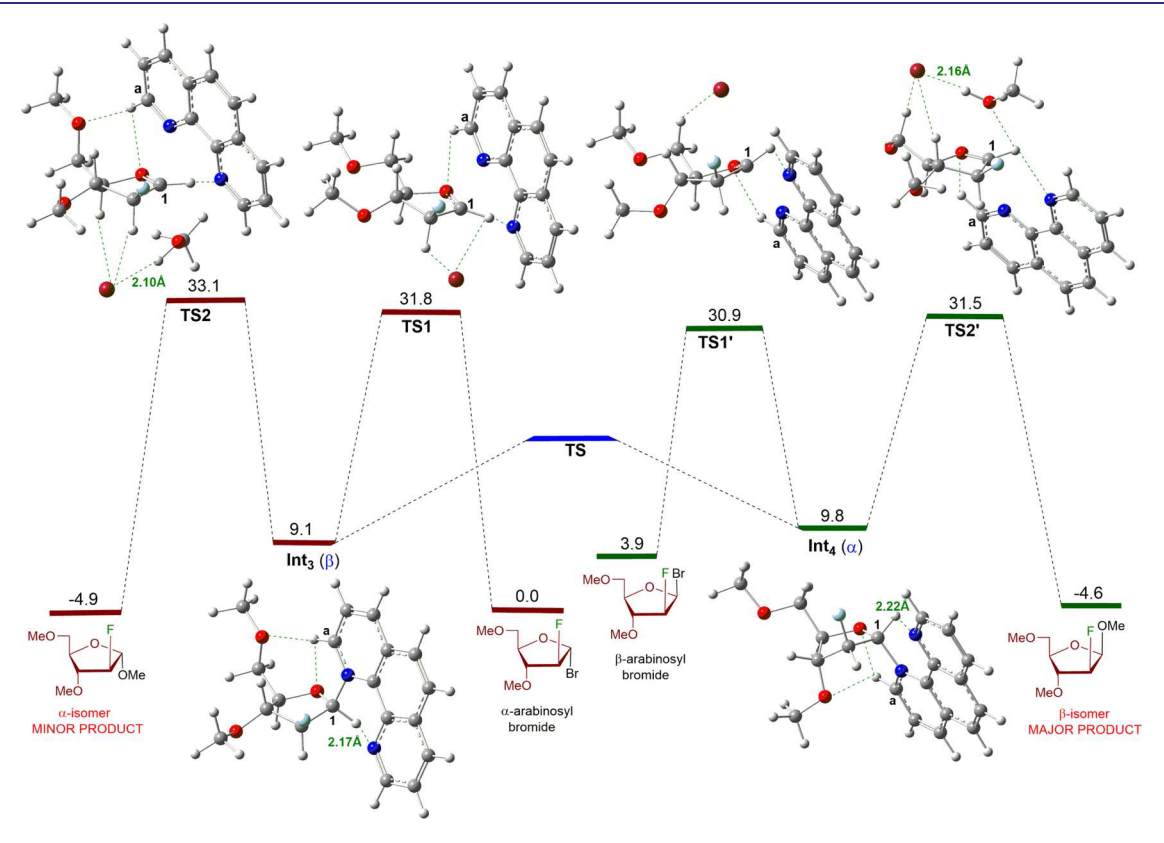


Figure 7. Energetic profile for the 2-fluoro-arabinofuranose substrate. Oxygen = red, nitrogen = blue, bromine = maroon, and fluorine = light blue. Hydrogen bonding interaction (green line). Free energies (kcal/mol) were computed with the Gaussian 16 quantum chemical program package 56 using the hybrid exchange—correlation functional M06-2X. 57,58

Figure 8. Possible mechanism for phenanthroline-catalyzed xylofuranosylation.

45β (Figure 4a). Meanwhile, increasing concentration of $\operatorname{Int}_2(\alpha)$ was also observed in the kinetic profile of the xylofuranosyl-phenanthrolinium intermediates (Figure 4b), while $\operatorname{Int}_1(\beta)$ concentration was maintained at a low level. These kinetic profiles suggested that the consumption rate of $\operatorname{Int}_1(\beta)$, which led to the major product 45α , was much faster than that of $\operatorname{Int}_2(\alpha)$. As more products were formed in the reaction, the consumption rate of $\operatorname{Int}_1(\beta)$ decreased, and a slight downward slope of product formation was observed at 7 h. This ratio of $\operatorname{Int}_1(\beta)$ and $\operatorname{Int}_2(\alpha)$ was maintained at 1:16 until the end of the reaction course (24 h), likely due to hydrolysis in the reaction.

On the other hand, in the reaction progress of 2-fluoro arabinofuranosyl bromide 42 (Figure 5), the ratio of intermediates $Int_3(\beta)$ and $Int_4(\alpha)$ only increased to 3:1 upon addition of primary alcohol 2 (Figure S10). Meanwhile, the α/β selectivity of the disaccharides 43 slowly decreased from 1:7 at 1 h to 1:5 at 6 h (Figures 5a and S9-S10). This 1:5 α/β ratio maintained until the end of the course of the reaction (20 h). Like the 2-fluoro-xylofuranosylation reaction, the kinetic profile of the 2-fluoro arabinofuranosylation also expressed apparent zero-order kinetics in the first 6 h. The disappearance rate of 42α was 24 times faster than that of 42β (Figure 5a), likely due to the higher concentration of starting material 42α , which further resulted in the higher concentration of $Int_3(\beta)$. However, unlike xylofuranosylation, the consumption rates of the two intermediates (Int₃(β) and Int₄(α), Figure 5b) in the arbinofuranosylation were similar, which eventually led to a lower selectivity in the products 43.

Interestingly, the kinetic profiles for both xylose and arabinose showed an accumulation (positive slope) of the intermediates (Figures 4b and 5b), suggesting that the rate-determining step takes place after the intermediates are formed. To provide

further insight into the mechanism and selectivity, density functional theory (DFT) calculations were employed to examine the key transition states and intermediates along the reaction pathway. To reduce the computational cost, both 3,5-dimethoxy-2-fluoro xylosyl and arabinosyl bromide donors as well as methanol were used as the model coupling partners for all calculations. The computed free energy profiles and the optimized structures of key intermediates and transition states are shown in Figures 6 and 7. The key findings are summarized below:

First, unlike the pyranose substrate, 50 we did not observe hydrogen bonding interaction between the C1-anomeric proton and the phenanthroline nitrogen with the furanose in our NMR studies. However, the phenanthroline nitrogen interacting with the anomeric H₁ proton (see Figures 6 and 7 as well as S17 and S18) still exists for all furanosyl phenanthrolinium ion species in our DFT calculations. For the xylose substrate, the C1-H···N distance for $Int_1(\beta)$ and $Int_2(\alpha)$ is 2.21 and 2.28 Å, respectively (Figures 6 and S17). In the case of the arabinose substrate, the C1-H···N distance for $Int_3(\beta)$ and $Int_4(\alpha)$ is 2.17 and 2.22 Å, respectively (Figures 7 and S18). Calculations further revealed hydrogen bonding interactions for both xylose and arabinose between a C-H vicinal to the bound nitrogen of phenanthroline (H_a) and the ring oxygen as well as C3- and C5-oxygen (Figures 6 and 7 as well as S17 and S18). To compare, there is only hydrogen bonding interaction between the C_{sp2} phenanthroline hydrogen H_a and the pyranose ring oxygen (Figure S19).⁴⁹ We hypothesize that the change seems likely to be in response to different steric demands placed on the rings by phenanthroline.

Second, we observed a hydrogen bonding interaction between Br⁻ ion and the MeOH proton, which is present in all TS2 structures—the nucleophilic attack by methanol onto the furanosyl phenanthrolinium ion intermediate—with the

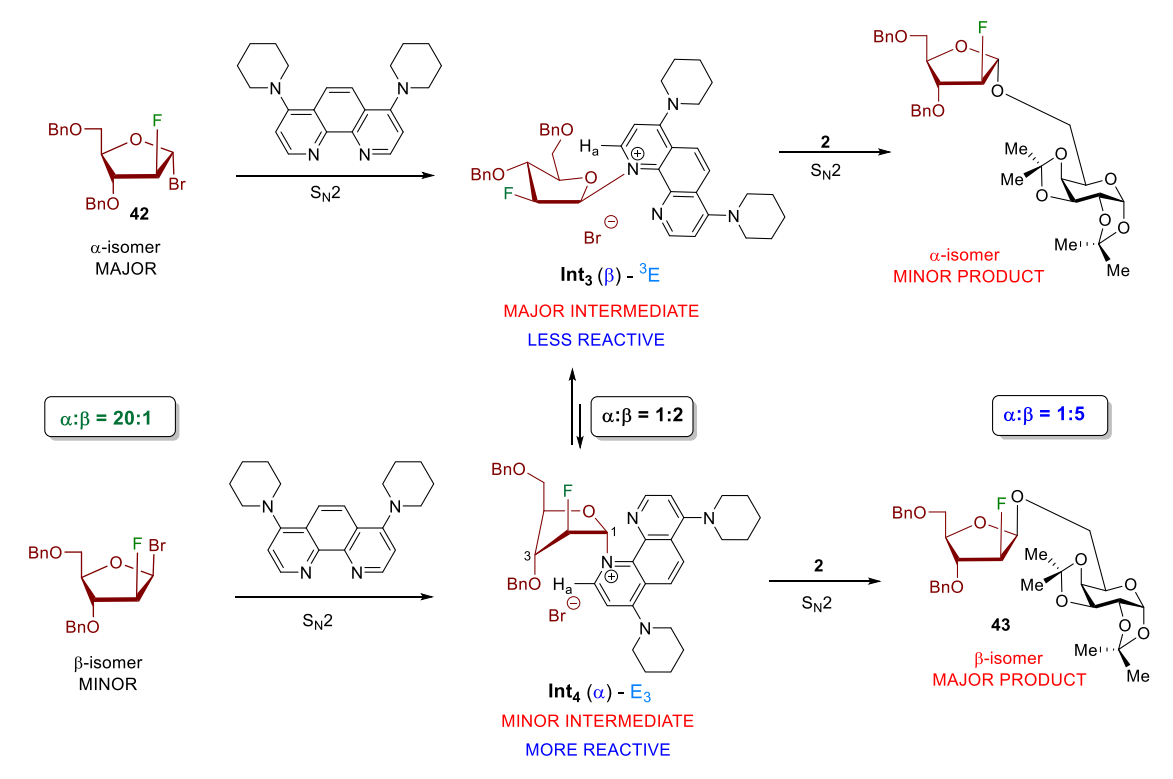


Figure 9. Possible mechanism for phenanthroline-catalyzed arabinofuranosylation.

MeOH···Br distance of 2.10–2.17 Å (Figures 6 and 7 as well as S21 and S23). The stabilizing effect of MeOH on Br¯ is very similar to that of the CH_2Cl_2 used to model the solvation of Br¯ (see the Supporting Information). There are additional hydrogen bonding interactions between Br- ions and the hydrogen (H_1) bound to the anomeric carbon since this center is sp² hybridized and a partial carbocation at both TS1 and TS2 transition states for the α-xylosyl isomer (Figures 6, S20, and S21) and at TS1 for the α-arabinosyl isomer (Figures 7 and S22). Weaker hydrogen bonding interactions between Br- ions and other $C_{\rm sp3}$ —H hydrogens of xylose and arabinose were also observed (Figures 6 and 7 as well as S20–S23).

Third, the energy barriers between the 1st and 2nd transition states for both xylose and arabinose substrates further support the stereochemical outcome of the 2-fluorofuranoside products. For the xylose substrate, the α -xylosyl bromide is 0.1 kcal/mol higher in energy than its corresponding β -xylosyl bromide starting material (Figure 6), which is consistent with our NMR result (α/β = 1:1.25, Scheme 2b). The difference between **TS2**- α and TS2'- β is 4.0 kcal/mol (Figure 6), supporting our experimental data that 1,2-cis- α -2-fluoroxyloside was obtained as a major product (α/β = 21:1). The difference in the **TS1** and **TS2** transition states for the major α -xyloside product is 0.4 kcal/mol, suggesting that the second step is the rate-limiting step. This computational observation matches our kinetic analysis (Figure 4b). Finally, the difference between $Int_1(\beta)$ and $Int_2(\alpha)$ is about 0.4 kcal/mol (see Figure 6 and discussion in the Supporting Information), and this calculation is consistent with the NMR result $(Int_1(\beta)/Int_2(\alpha) = 2:1$, Scheme 3a).

In the case of arabinose, the calculated β -arabinosyl bromide is 3.9 kcal/mol higher in energy than its corresponding α -arabinosyl bromide (Figure 7), and this computational observation matches our NMR result ($\alpha/\beta = 20:1$, Scheme 2a). Our experimental data (Scheme 3b and Figure 5) shows that $\text{Int}_3(\beta)$ and $\text{Int}_4(\alpha)$ were formed in a ratio of 2:1-3:1 β/α

mixture. The DFT calculations find a difference of 0.7 kcal/mol between ${\rm Int_3}(\beta)$ and ${\rm Int_4}(\alpha)$ (see Figure 7), which is consistent with the NMR result. The calculated difference in the TS1' and TS2' transition states for the major β -arabinoside product is 0.6 kcal/mol, suggesting that the second step is the rate-limiting step.

Finally, the rapid formation of the 2-fluorofuranosyl phenanthrolium intermediates observed by NMR studies (Scheme 3, and Figures 4–5) suggests that the barriers for interconversion of the α - and β -phenanthrolium intermediates for both xylose and arabinose substrates are significantly lowered compared to **TS1** and **TS2** (Figures 6 and 7). However, the transition states for the interconversion of the intermediates have not been found in the DFT calculations.

Based on the NMR data (Scheme 3a), kinetic profile (Figure 4), and computational results (Figure 6) for xylofuranosyl bromide donor 44, we propose the following mechanistic rationale for the observed α -1,2-cis stereochemistry (Figure 8). Since α - and β -isomers of xylofuranosyl bromide 44 exist as a 1:1.25 mixture, displacement of their anomeric bromide leaving group with NPhen via an S_N 2-like pathway would generate ${}^3E \beta$ phenanthrolinium ion conformer $Int_1(\beta)$ and E_3 α -phenanthrolinium ion conformer $Int_2(\alpha)$, respectively, with the preference of the $Int_1(\beta)$ intermediate. Calculations predict that $Int_2(\alpha)$ is less stable than $Int_1(\beta)$ (0.4 kcal/mol, Figure 6), likely due to eclipsing interaction between C2-F and C1-N in $Int_2(\alpha)$ (Figure S17). Nucleophilic attack of alcohol acceptor 2 onto $Int_1(\beta)$, via an S_N 2-like pathway, would provide the α xyloside product 45. To obtain high levels of 1,2-cis selectivity, a Curtin-Hammett situation must be established such that equilibration of $Int_1(\beta)$ and $Int_2(\alpha)$ is rapid and much faster than the subsequent nucleophilic attack. The hypothesis that the rate-determining step takes place after the phenanthrolinium intermediates are formed was confirmed by kinetic analysis (Figure 4b) and computational observation (Figure 6). It is also

observed that $\operatorname{Int}_1(\beta)$ is not only the more stable intermediate than $\operatorname{Int}_2(\alpha)$ by 0.4 kcal/mol (Figure 6) but also is the faster-reacting conformer (Figure 4b). Indeed, the calculated TS2 transition state for the formation of the α -xyloside product resulting from $\operatorname{Int}_1(\beta)$ is 4.0 kcal/mol, more favorable than the analogous formation of the β -xyloside product (Figure 6). Collectively, the α -1,2-cis xyloside product 45 resulting from the nucleophilic attack of alcohol 2 onto the major intermediate $\operatorname{Int}_1(\beta)$ should prevail and will not reflect the equilibrium distribution of $\operatorname{Int}_1(\beta)$ and $\operatorname{Int}_2(\alpha)$.

In the case of arabinose, the NMR data illustrated in Scheme 3b and Figures S8-S9, the kinetic profile (Figure 5), and DFT calculations (Figure 7) for arabinofuranosyl bromide suggest that (1) the donor anomeric composition would not reflect the intermediate distribution and (2) although $Int_4(\alpha)$ is the minor intermediate observed by both NMR study (Scheme 3b and Figure 5b) and DFT calculation (Figure 7), it is the fast-reacting conformer that reacts with alcohol acceptor to form the major β -1,2-cis-arabinoside product (see the proposed mechanism in Figure 9). Kinetic analysis (Figure 5b) shows that the rate of the nucleophilic substitution of $\operatorname{Int}_4(\alpha)$ is also faster than that of the more stable one $\operatorname{Int}_3(\beta)$. As a result, as soon as $\operatorname{Int}_4(\alpha)$ is consumed, it is replenished from $Int_3(\beta)$, as the energy barrier for interconversion of Int, and Int, is low. The difference of the energy barrier for the two transition states (TS2- α and TS2'- β) is about 1.6 kcal/mol (Figure 7), further supporting the experimental result that a mixture of 1,2-cis- and 1,2-transarabinoside products (5:1) was obtained in the reaction.

CONCLUSIONS

A phenanthroline-catalyzed stereoselective furanosylation is developed to achieve access to the challenging 1,2-cis furanosidic linkages. Substitution of xylofuranosyl bromide donor with a variety of primary and secondary hydroxyl acceptors affords α -1,2-cis linked products in high yields and with excellent levels of cis/trans diastereoselectivity. This phenanthroline catalysis method is also applicable to other furanosyl donors. While the reaction of D-arabinofuranosyl bromide with a variety of hydroxyl acceptors affords β -1,2-cis linked products in good to high yields and selectivity, furanosylation of D-ribofuranosyl and L-arabinofuranosyl bromide donors provides selective access to α -1,2-cis linked products. Experiments with 2-fluoro-xylofuranosyl and -arabinofuranosyl bromide donors indicate that furanosyl donor anomeric composition is not responsible for the reaction selectivity. Importantly, the furanosylation reaction is unlikely to proceed through a stereospecific substitution. NMR experiments, kinetic profile, and DFT calculations indicate that the second transition state—the nucleophilic attack of alcohol onto the faster-reacting phenanthrolinium ion intermediate determines the stereochemistry of the product. Collectively, the results obtained highlight the unique features of phenanthroline to catalyze the highly stereoselective furanosylation reactions. The utility of this new method is currently extending to other carbohydrate electrophiles.

ASSOCIATED CONTENT

Supporting Information

The Supporting Information is available free of charge at https://pubs.acs.org/doi/10.1021/jacs.2c02063.

Full experimental procedures and characterization data for all new compounds, NMR spectra of new compounds, and DFT data (PDF)

AUTHOR INFORMATION

Corresponding Authors

- H. Bernhard Schlegel Department of Chemistry, Wayne State University, Detroit, Michigan 48202, United States;
 - orcid.org/0000-0001-7114-2821; Email: hbs@chem.wayne.edu
- Hien M. Nguyen Department of Chemistry, Wayne State University, Detroit, Michigan 48202, United States;
- orcid.org/0000-0002-7626-8439; Email: hmnguyen@wayne.edu

Authors

Hengfu Xu — Department of Chemistry, Wayne State University, Detroit, Michigan 48202, United States

Richard N. Schaugaard – Department of Chemistry, Wayne State University, Detroit, Michigan 48202, United States; orcid.org/0000-0003-3351-8810

Jiayi Li – Department of Chemistry, Wayne State University, Detroit, Michigan 48202, United States

Complete contact information is available at: https://pubs.acs.org/10.1021/jacs.2c02063

Author Contributions

[†]R.N.S. and J.L. contributed equally to this work.

Notes

The authors declare no competing financial interest.

ACKNOWLEDGMENTS

This research is supported by NIH (R01GM098285 for H.M.N.) and NSF (CHE1856437 for H.B.S.). The authors thank the Wayne State University Lumigen Center for instrumental assistance and the Wayne State University Grid for computing resources.

REFERENCES

- (1) Marino, C.; Gallo-Rodriguez, C.; Lederkremer, R. M. d. Galactofuranosyl-containing Glycans: Occurrence, Synthesis and Biochemistry. In *Glycans: Biochemistry, Characterization and Applications*; Mora-Montes, H. M., Ed.; Nova Science Publishers, Inc.: Hauppauge, NY, 2012; pp 207–268.
- (2) Richards, M. R.; Lowary, T. L. Chemistry and biology of galactofuranose-containing polysaccharides. *Chembiochem* **2009**, *10*, 1920–1938.
- (3) Tefsen, B.; van Die, I. Glycosyltransferases in chemo-enzymatic synthesis of oligosaccharides. *Methods Mol. Biol.* **2013**, *1022*, 357–367.
- (4) Lowary, T. L. Synthesis and conformational analysis of arabinofuranosides, galactofuranosides and fructofuranosides. *Curr. Opin. Chem. Biol.* **2003**, *7*, 749–756.
- (5) Imamura, A.; Lowary, T. Chemical Synthesis of Furanose Glycosides. *Trends Glycosci. Glycotechnol.* **2011**, 23, 134–152.
- (6) Gallo-Rodriguez, C.; Kashiwagi, G. A. Selective Glycosylations with Furanosides. In *Selective Glycosylations: Synthetic Methods and Catalysts*; Bennett, C. S., Eds.; 2017; pp 297–326.
- (7) Angala, S. K.; Belardinelli, J. M.; Huc-Claustre, E.; Wheat, W. H.; Jackson, M. The cell envelope glycoconjugates of Mycobacterium tuberculosis. *Crit. Rev. Biochem. Mol. Biol.* **2014**, *49*, 361–399.
- (8) Lowary, T. L. Twenty Years of Mycobacterial Glycans: Furanosides and Beyond. *Acc. Chem. Res.* **2016**, *49*, 1379–1388.
- (9) Crick, D. C.; Mahapatra, S.; Brennan, P. J. Biosynthesis of the arabinogalactan-peptidoglycan complex of Mycobacterium tuberculosis. *Glycobiology* **2001**, *11*, 107r–118r.
- (10) Brennan, P. J.; Nikaido, H. The envelope of mycobacteria. *Annu. Rev. Biochem.* **1995**, *64*, 29–63.

- (11) Lowary, T. L. Recent Progress Towards the Identification of Inhibitors of Mycobacterial Cell Wall Polysaccharide Biosynthesis. *Mini-Rev. Med. Chem.* **2003**, *3*, 689–702.
- (12) Pedersen, L. L.; Turco, S. J. Galactofuranose metabolism: a potential target for antimicrobial chemotherapy. *Cell. Mol. Life Sci.* **2003**, *60*, 259–266.
- (13) Taha, H. A.; Richards, M. R.; Lowary, T. L. Conformational Analysis of Furanoside-Containing Mono- and Oligosaccharides. *Chem. Rev.* 2013, 113, 1851–1876.
- (14) Zhu, X. M.; Kawatkar, S.; Rao, Y.; Boons, G. J. Practical approach for the stereoselective introduction of beta-arabinofuranosides. *J. Am. Chem. Soc.* **2006**, *128*, 11948–11957.
- (15) Crich, D.; Pedersen, C. M.; Bowers, A. A.; Wink, D. J. On the use of 3,5-O-benzylidene and 3,5-O-(di-tert-butylsilylene)-2-O-benzylar-abinothiofuranosides and their sulfoxides as glycosyl donors for the synthesis of beta-arabinofuranosides: Importance of the activation method. *J. Org. Chem.* **2007**, 72, 1553–1565.
- (16) Wang, Y. X.; Maguire-Boyle, S.; Dere, R. T.; Zhu, X. M. Synthesis of beta-D-arabinofuranosides: stereochemical differentiation between D- and L-enantiomers. *Carbohydr. Res.* **2008**, *343*, 3100–3106.
- (17) Imamura, A.; Lowary, T. L. beta-Selective Arabinofuranosylation Using a 2,3-O-Xylylene-Protected Donor. *Org. Lett.* **2010**, *12*, 3686–3689
- (18) Tilve, M. J.; Gallo-Rodriguez, C. Glycosylation studies on conformationally restricted 3,5-O-(di-tert-butylsilylene)-D-galactofuranosyl trichloroacetimidate donors for 1,2-cis alpha-D-galactofuranosylation. *Carbohydr. Res.* **2011**, 346, 2838–2848.
- (19) Zhang, L.; Shen, K.; Taha, H. A.; Lowary, T. L. Stereocontrolled Synthesis of alpha-Xylofuranosides Using a Conformationally Restricted Donor. *J. Org. Chem.* **2018**, *83*, 7659–7671.
- (20) Bamhaoud, T.; Sanchez, S.; Prandi, J. 1,2,5-ortho esters of Darabinose as versatile arabinofuranosidic building blocks. Concise synthesis of the tetrasaccharidic cap of the lipoarabinomannan of Mycobacterium tuberculosis. *Chem. Commun.* **2000**, 659–660.
- (21) Sanchez, S.; Bamhaoud, T.; Prandi, J. A comprehensive glycosylation system for the elaboration of oligoarabinofuranosides. *Tetrahedron Lett.* **2000**, *41*, 7447–7452.
- (22) Ishiwata, A.; Munemura, Y.; Ito, Y. NAP ether mediated intramolecular aglycon delivery: A unified strategy for 1,2-cis-glycosylation. *Eur. J. Org. Chem.* **2008**, 2008, 4250–4263.
- (23) Argunov, D. A.; Krylov, V. B.; Nifantiev, N. E. Convergent synthesis of isomeric heterosaccharides related to the fragments of galactomannan from Aspergillus fumigatus. *Org. Biomol. Chem.* **2015**, 13, 3255–3267.
- (24) Lee, Y. J.; Lee, K.; Jung, E. H.; Jeon, H. B.; Kim, K. S. Acceptor-dependent stereoselective glycosylation: 2'-CB glycoside-mediated direct beta-D-arabinofuranosylation and efficient synthesis of the octaarabinofuranoside in mycobacterial cell wall. *Org. Lett.* **2005**, *7*, 3263–3266.
- (25) Liu, Q. W.; Bin, H. C.; Yang, J. S. beta-Arabinofuranosylation Using 5-O-(2-Quinolinecarbonyl) Substituted Ethyl Thioglycoside Donors. *Org. Lett.* **2013**, *15*, 3974–3977.
- (26) Gadikota, R. R.; Callam, C. S.; Wagner, T.; Del Fraino, B.; Lowary, T. L. 2,3-anhydro sugars in glycoside bond synthesis. Highly stereoselective syntheses of oligosaccharides containing alpha- and beta-arabinofuranosyl linkages. *J. Am. Chem. Soc.* **2003**, *125*, 4155–4165.
- (27) Gadikota, R. R.; Callam, C. S.; Lowary, T. L. Stereocontrolled synthesis of 2,3-anhydro-beta-D-lyxofuranosyl glycosides. *Org. Lett.* **2001**, 3, 607–610.
- (28) Mereyala, H. B.; Hotha, S.; Gurjar, M. K. Synthesis of pentaarabinofuranosyl structure motif a of Mycobacterium tuberculosis. *Chem. Commun.* **1998**, 685–686.
- (29) Désiré, J.; Prandi, J. Synthesis of methyl beta-D-arabinofuranoside 5-[1D (and L)-myo-inositol 1-phosphate], the capping motif of the lipoarabinomannan of Mycobacterium smegmatis. *Carbohydr. Res.* 1999, 317, 110–118.

- (30) Subramaniam, V.; Lowary, T. L. Synthesis of oligosaccharide fragments of mannosylated lipoarabinomannan from Mycobacterium tuberculosis. *Tetrahedron* **1999**, *55*, 5965–5976.
- (31) D'Souz, F. W.; Lowary, T. L. The first total synthesis of a highly branched arabinofuranosyl hexasaccharide found at the nonreducing termini of mycobacterial arabinogalactan and lipoarabinomannan. *Org. Lett.* **2000**, *2*, 1493–1495.
- (32) Yin, H. F.; D'Souza, F. W.; Lowary, T. L. Arabinofuranosides from mycobacteria: Synthesis of a highly branched hexasaccharide and related fragments containing beta-axabinofuranosyl residues. *J. Org. Chem.* **2002**, *67*, 892–903.
- (33) Joe, M.; Sun, D.; Taha, H.; Completo, G. C.; Croudace, J. E.; Lammas, D. A.; Besra, G. S.; Lowary, T. L. The 5-deoxy-5-methylthio-xylofuranose residue in mycobacterial lipoarabinomannan. Absolute stereochemistry, linkage position, conformation, and immunomodulatory activity. J. Am. Chem. Soc. 2006, 128, 5059–5072.
- (34) Thadke, S. A.; Mishra, B.; Hotha, S. Facile Synthesis of beta- and alpha-Arabinofuranosides and Application to Cell Wall Motifs of M. tuberculosis. *Org. Lett.* **2013**, *15*, 2466–2469.
- (35) Erkkilä, A.; Majander, I.; Pihko, P. M. Iminium catalysis. *Chem. Rev.* **2007**, 107, 5416–5470.
- (36) Mukherjee, S.; Yang, J. W.; Hoffmann, S.; List, B. Asymmetric enamine catalysis. *Chem. Rev.* **2007**, *107*, 5471–5569.
- (37) Wurz, R. P. Chiral dialkylaminopyridine catalysts in asymmetric synthesis. *Chem. Rev.* **2007**, *107*, 5570–5595.
- (38) Gaunt, M. J.; Johansson, C. C. C. Recent developments in the use of catalytic asymmetric ammonium enolates in chemical synthesis. *Chem. Rev.* **2007**, *107*, 5596–5605.
- (39) Enders, D.; Niemeier, O.; Henseler, A. Organocatalysis by Nheterocyclic, carbenes. *Chem. Rev.* **2007**, *107*, 5606–5655.
- (40) Hashimoto, T.; Maruoka, K. Recent development and application of chiral phase-transfer catalysts. *Chem. Rev.* **2007**, *107*, 5656–5682.
- (41) Atodiresei, I.; Schiffers, I.; Bolm, C. Stereoselective anhydride openings. *Chem. Rev.* **2007**, *107*, 5683–5712.
- (42) Doyle, A. G.; Jacobsen, E. N. Small-molecule H-bond donors in asymmetric catalysis. *Chem. Rev.* **2007**, *107*, 5713–5743.
- (43) Akiyama, T. Stronger bronsted acids. Chem. Rev. 2007, 107, 5744-5758.
- (44) Davie, E. A. C.; Mennen, S. M.; Xu, Y. J.; Miller, S. J. Asymmetric catalysis mediated by synthetic peptides. *Chem. Rev.* **2007**, *107*, 5759–5812.
- (45) Kamber, N. E.; Jeong, W.; Waymouth, R. M.; Pratt, R. C.; Lohmeijer, B. G. G.; Hedrick, J. L. Organocatalytic ring-opening polymerization. *Chem. Rev.* **2007**, *107*, 5813–5840.
- (46) McGarrigle, E. M.; Myers, E. L.; Illa, O.; Shaw, M. A.; Riches, S. L.; Aggarwal, V. K. Chalcogenides as organocatalysts. *Chem. Rev.* **2007**, *107*, 5841–5883.
- (47) Mayfield, A. B.; Metternich, J. B.; Trotta, A. H.; Jacobsen, E. N. Stereospecific Furanosylations Catalyzed by Bis-thiourea Hydrogen-Bond Donors. *J. Am. Chem. Soc.* **2020**, *142*, 4061–4069.
- (48) Yu, F.; Li, J. Y.; DeMent, P. M.; Tu, Y. J.; Schlegel, H. B.; Nguyen, H. M. Phenanthroline-Catalyzed Stereoretentive Glycosylations. *Angew. Chem., Int. Ed.* **2019**, *58*, 6957–6961.
- (49) DeMent, P. M.; Liu, C. L.; Wakpal, J.; Schaugaard, R. N.; Schlegel, H. B.; Nguyen, H. M. Phenanthroline-Catalyzed Stereoselective Formation of alpha-1,2-cis 2-Deoxy-2-Fluoro Glycosides. *Acs Catal* **2021**, *11*, 2108–2120.
- (50) Li, J. Y.; Nguyen, H. M. A Mechanistic Probe into 1,2-cis Glycoside Formation Catalyzed by Phenanthroline and Further Expansion of Scope. *Adv. Synth. Catal.* **2021**, *363*, 4054–4066.
- (51) Lemieux, R. U.; Hendriks, K. B.; Stick, R. V.; James, K. Halide Ion Catalyzed Glycosidation Reactions Syntheses of Alpha-Linked Disaccharides. *J. Am. Chem. Soc.* **1975**, *97*, 4056–4062.
- (52) Lammers, T.; Sofias, A. M.; van der Meel, R.; Schiffelers, R.; Storm, G.; Tacke, F.; Koschmieder, S.; Brummendorf, T. H.; Kiessling, F.; Metselaar, J. M. Dexamethasone nanomedicines for COVID-19. *Nat. Nanotechnol.* **2020**, *15*, 622–624.

- (53) Weissmann, M.; Bhattacharya, U.; Feld, S.; Hammond, E.; Ilan, N.; Vlodavsky, I. The heparanase inhibitor PG545 is a potent antilymphoma drug: Mode of action. *Matrix Biol.* **2019**, *77*, 58–72.
- (54) Larsen, C. H.; Ridgway, B. H.; Shaw, J. T.; Smith, D. M.; Woerpel, K. A. Stereoselective C-glycosylation reactions of ribose derivatives: Electronic effects of five-membered ring oxocarbenium ions. *J. Am. Chem. Soc.* **2005**, *127*, 10879–10884.
- (55) Aiguabella, N.; Holland, M. C.; Gilmour, R. Fluorine-directed 1,2-trans glycosylation of rare sugars. *Org. Biomol. Chem.* **2016**, *14*, 5534–5538.
- (56) Frisch, M. J.; Trucks, G. W.; Schlegel, H. B.; Scuseria, G. E.; Robb, M. A.; Cheeseman, J. R.; Scalmani, G.; Barone, V.; Petersson, G. A.; Nakatsuji, H.; Li, X.; Caricato, M.; Marenich, A. V.; Bloino, J.; Janesko, B. G.; Gomperts, R.; Mennucci, B.; Hratchian, H. P.; Ortiz, J. V.; Izmaylov, A. F.; Sonnenberg, J. L.; Williams; Ding, F.; Lipparini, F.; Egidi, F.; Goings, J.; Peng, B.; Petrone, A.; Henderson, T.; Ranasinghe, D.; Zakrzewski, V. G.; Gao, J.; Rega, N.; Zheng, G.; Liang, W.; Hada, M.; Ehara, M.; Toyota, K.; Fukuda, R.; Hasegawa, J.; Ishida, M.; Nakajima, T.; Honda, Y.; Kitao, O.; Nakai, H.; Vreven, T.; Throssell, K.; Montgomery, J. A., Jr.; Peralta, J. E.; Ogliaro, F.; Bearpark, M. J.; Heyd, J. J.; Brothers, E. N.; Kudin, K. N.; Staroverov, V. N.; Keith, T. A.; Kobayashi, R.; Normand, J.; Raghavachari, K.; Rendell, A. P.; Burant, J. C.; Iyengar, S. S.; Tomasi, J.; Cossi, M.; Millam, J. M.; Klene, M.; Adamo, C.; Cammi, R.; Ochterski, J. W.; Martin, R. L.; Morokuma, K.; Farkas, O.; Foresman, J. B.; Fox, D. J. Gaussian 16, Rev. C.01, Wallingford, CT, 2016.
- (57) Wang, Y.; Verma, P.; Jin, X.; Truhlar, D. G.; He, X. Revised M06 density functional for main-group and transition-metal chemistry. *Proc. Natl. Acad. Sci. U.S.A.* **2018**, *115*, 10257–10262.
- (58) Zhao, Y.; Truhlar, D. G. The M06 suite of density functionals for main group thermochemistry, thermochemical kinetics, noncovalent interactions, excited states, and transition elements: two new functionals and systematic testing of four M06-class functionals and 12 other functionals. *Theor. Chem. Acc.* 2008, 120, 215–241.